Washcoating of low surface area cerium oxide on complex geometry substrates

Riccardo Balzarotti Cinzia Cristiani Saverio Latorrata and Alessandro Migliavacca

Politecnico di Milano, Dip artimento di Chimica, Materiali e Ingegneria Chimica "G. Natta", Milano, Italy

Introduction

Thin oxide layer deposition is a well-known research topic, cross-sectorial to many innovation fields. Catalysis is continuously in search of new systems in order to achieve improvements in process intensification (Tronconi and Groppi 2009). In this view, significant changes occurred in recent years, with the employment of high complexity morphological supports for catalytic application. Among them, solid open cell foams have been widely investigated due to their geometrical characteristics, able to maximize interfacial areas and, therefore, to enhance the rates of fluid/solid mass transfer processes. They also grant an improvement in energy efficiency (lower pressure drop) because of high porosities. Open-cell foams, also named sponges, have cellular structures where space is filled by filaments (struts), thus forming a continuous network which encloses cavities (cells), interconnected by open windows (pores).

Several methods are proposed in the literature to deposit the catalytic layer on the surface of the structured substrates (Meille 2006), intended as ceramic (Al_2O_3, cordierite, SiC, etc.) or metallic (e.g., stainless steel, aluminum, copper, etc.). Wet coating is the easiest and most versatile technique for pro-ducing coatings by depositing a liquid-like precursor onto a substrate that is converted to the desired coating material by subsequent post-treatment steps (Aegerter and Mennig 2004). Among these methods, dip-coating from a sol or a slurry liquid phase is the most cost-effective and the simplest one to be used in practice (Montebelli et al. 2014).

In particular, dip-coating consists in filling the voids of the substrate with a powder suspension (or a sol–gel dispersion) by dipping. Then, the filled substrate is withdrawn from the liquid-like material at controlled speed. Using this process, opposite forces act on the fluid film during the extraction step: the gravitational force, attracting the film downward, and the viscous force which hinders its sliding (Middleman 1977; Brinker and Scherer 1990). As a result, deposited film thickness depends on the balance between fluid viscosity and substrate withdrawal speed (Valentini et al. 2001). Therefore, the control of slurry rheological behavior and of withdrawal velocity is crucial to determine the coated layer properties.

The use of the suspension method is quite common in catalytic application and it can be applied on either the morphologic support or the finished catalyst itself. A properly sized powder, binder, dispersant (typically an acid), and a solvent are the typical formulation components, whose concentrations may largely vary, primarily depending on the nature of the solid to be suspended and on the required rheological behavior.

Suspension formulation (e.g., water/powder ratio, acid/powder ratio, dispersant content), and thereby its rheological behavior strongly affect slurry stability and coating perfor-mances. Indeed, low viscosity values promote good adhesion but low loadings are obtained, whereas high viscosity induces high catalyst loading but poor adhesion (Valentini et al. 2001).

Acids are typically employed as dispersants to stabilize slurries and to properly tune their rheology via powder surface charging (SC). In this case, operating pH directly influences rheological behavior and suspension stability. A similar effect is found for the solid concentration. Generally, once the water/powder ratio is fixed, more acidic suspensions result in higher viscosity, due to a higher amount of suspended powder and enhanced liquid to powder interaction (Valentini et al. 2001; Visconti et al. 2009). However, a threshold value, corresponding

Riccardo Balzarotti-riccardo.balzarotti@polimi.it Dipartimento di Chimica, Materiali e Ingegneria Chimica "Giulio Natta", Piazza Leonardo da Vinci 32, Milano, 20133, Italy.

to the maximum SC of that particle, exists, beyond which no further improvement in the solid dispersion can be achieved. Accordingly, an increase in the viscosity, observed upon further acid addition, has been related to acid-catalyzed cross-linking reactions inside the slurry. The evaluation of the SC needed to optimize the amount of acid to be added to the slurry can be done via acid titration (Cristiani et al. 2009) or zeta-potential measurements (Rodriguez et al. 2009).

In some cases, however, acidic additions to the slurry are not suitable. Indeed, acidic attacks may cause significant chemical transformations of the catalyst powder. Therefore, alternative routes to promote slurry stability and to obtain rheological behavior suitable for deposition have to be found.

For instance, long-chain surfactants containing hydrophilic and hydrophobic groups, like polyethylene glycol, polyethylene imine, and Triton X-100 (Meille et al. 2005) adsorb on the catalyst surface, leading to steric stabilization of the slurry. Some of them are also used as rheology modifiers like isopropyl alcohol, polyvinyl alcohol (PVA), polyvinylpyrrolidone, ammonium methacrylate, and methylhydroxyethyl cellulose (Won et al. 2006; Germani et al. 2007; Phan et al. 2011).

After formulation selection, slurry components are usually milled in a rotating jar at constant rate in presence of zirconium oxide spheres as grinding bodies (Bravo et al. 2004; Cristiani et al. 2009; Visconti et al. 2009), to reduce powder particle size. This process typically leads to satisfactory adhesion and endurance of the coating material (Agrafiotis, Tsetsekou, and Ekonomakou 1999).

Post-deposition procedures, generally thermal treatments, are then performed to consolidate and to anchor the coating layer (Valentini et al. 2001).

As introduced before, SC is a well-known method to obtain stable oxide dispersions; it consists in powder SC by chemical reactions, in order to exploit particle repulsion and achieve a proper system stabilization. However, in the case of low surface area (SA) oxides, where measured SC is near to zero at any pH, this method cannot be applied. Indeed, very low or at least no interactions between powder surface and protons will occur, thus preventing any electrostatic repulsion (Valentini et al. 2001; Visconti et al. 2009). Moreover, the use of acid is not allowed in case of etching effects that could change the nature of the suspending powders.

Many good papers have been devoted both to slurry formulation and to washcoating process (Montebelli et al. 2014). However, a lack of information dealing with formulation effect on final washcoat deposited via the slurry route on ceramic foams is present, in particular, when low surface oxides are used. In addition to that, the slurry formulation stability to coating property correlation has not to be fully clarified.

Among others, cerium oxide is a support of choice for many different processes (Hosokawa et al. 2005). In particular, CeO_2 is widely used as support for reforming catalysts due to its oxygen mobility and storage capacity (Maupin et al. 2011). Moreover, cerium oxide can lead to the formation of metal-carrier redox couples, which can help in limiting carbon production (Vita et al. 2015). All these properties make cerium oxide a good candidate for transition metal-based catalysts with relatively high activity, fairly good stability, and lower cost than noble metals (Shan et al. 2003).

Accordingly, the purpose of this work is to study formulations and procedures to produce thin ceramic layers using a commercial cerium oxide powder, selected as model of low SA oxides (SC near to zero), on substrates of complex geometry such as ceramic open cell foams.

For reasons stated, acid-free formulations based on water (H), glycerol (G), and PVA were studied to disperse and stabilize powders via steric-like interaction. Thus, a dispersion route that implied a milling process and proper ratios among the components was experienced. PVA was used as viscosity modulator in order to control viscosity and to enhance system stability. Slurry rheology was related to the PVA content and slurry composition. Furthermore, the effects of both coating procedure and thermal treatments on final coating load and adhesion were also assessed. The final goal was to understand how homogeneous coverage, no pore clogging, and good adhesion performances could be obtained via proper tuning of the starting powder suspension.

Experimental

Materials

Yttria-stabilized zirconia alumina (YZA) foams with 20, 30, and 40 pore per inch density (PPI) (Selee Corporation, Hendersonville, NC, USA) were used as geometrical support.

Commercial cerium oxide (CeO_2, supplied by Sigma-Aldrich, Milan, Italy) was used as a representative sample of low SA powders. It consists of a fluorite structure with a SA of 3 $m^2\ g^{-1}$ and a pore volume (Vp) of 0.4 $cm^3\ g^{-1}$. No SCSC capacity (C m^{-2}), measured according to the procedure reported in the literature (Valentini et al. 2001), was found.

Glycerol (G) (87% w/w water solution, Sigma-Aldrich) was used as dispersant while PVA (Mowiol, Sigma-Aldrich), was used as plasticizer (Zhang et al. 2012). Distilled water (H) was used as solvent.

Procedures

Slurry preparation

In this work, the final slurry was obtained according to a procedure already developed; details are reported elsewhere (Valentini et al. 2001). In a typical experiment, PVA, used as plasticizer, was dissolved in distilled water under magnetic stirring at 85°C; following G, used as dispersant, was added under magnetic stirring for obtaining the final liquid media, suitable for powder dispersion. CeO_2 powder was added to the solution thus obtained; then it was poured in a polyethylene jar and ball-milled (ZrO_2 grinding bodies) for 24 h at constant rotation rate (50 rpm).

Components ratios will be specified along the text; thus, in the following, the studied samples will be identified by a label indicating their main components.

Coating deposition

Before coating deposition, foams were cleaned with acetone for 30 min in an ultrasound bath.

In order to reduce foaming, a sonication pretreatment was performed for 30 min on the CeO_2 slurry. Coating deposition

was carried out via dip-coating technique, using a self-made dip-coater with tunable withdrawal velocity. Velocities between 6 and 31 cm min^{-1} were tested and held constant during sample extraction step. Coated samples were then flash dried for 6 min at 350°C in a sealed oven. Following, a calci-nation process was performed at 900°C for 10 h, using a 2°C min^{-1} rate for both heating and cooling ramps.

Characterization

Powder particle size was assessed by laser granulometry by using a CILAS 1180 instrument (Compagnie Industrielle des Lasers, Orléans, France).

Dispersions rheological properties were assessed by means of a rotational rheometer (Stresstech 550, Reologica Instruments, Bordentown, NJ, USA) using parallel disc geometry plates (40 mm diameter, 1 mm gap). Dynamic viscosities were investigated in the shear rates range 10^{-2} to $10^{3}\,s^{-1}$.

Differential Thermal Analysis-Thermogravimetry (DTA-TG) were performed by using an Extar 6000, Seiko Instrument. Analyses were performed in air from room temperature (r.t.) up to 500°C, with a heating rate of 5°C min^{-1}.

In order to evaluate dispersion stability, sedimentation tests were performed according to literature (Gu et al. 2003). In a typical test, dispersions were poured in a test tube and the initial height (H_0) was measured: then, the decreasing height (H_0–x) was measured at fixed time intervals and the residual height (H) was evaluated. Dispersion stability (H/H_0) was calculated according to Equation (1), where calculated values can vary from 1 (perfect stability) to 0 (complete settling):

$$\text{Stability} = \frac{H_0 - x}{H_0} = \frac{H}{H_0} \quad (1)$$

For the first 5 h, height decrease was measured every 15 min (short-term stability); furthermore, values at about 3000 min and about 9000 min were noted down in order to assess long-term stability.

Coating load was determined by weighting the bare and the coated support before and after both flash drying and high-temperature thermal treatments.

Coating adhesion was evaluated by sonication for 30 min in petroleum ether bath according to literature (Cristiani et al. 2012).

Coating layer homogeneity and morphology were evaluated by means of an optical microscope (Olympus, SZ-CTV).

Results and discussion

Slurry formulation

Slurry formulation is one of the key points in washcoating process. Component ratios are macroscopic parameters that can be easily handled to tune microscopic scale parameters, such as morphology, homogeneity, and adhesion of the coated layer.

Two main targets have to be achieved in slurry preparation: rheological behavior and stability. Both of them can be obtained by a wise mixing of powder, dilutant, and additives required for powder dispersion. On this basis, both time stability and rheology of CeO_2 slurries were studied.

Slurry stability assessment

As reported in literature (Agrafiotis, Tsetsekou, and Ekonomakou 1999; Valentini et al. 2001), slurry stability depends on many factors, such as powder concentration, chemical nature of the dispersant, and particle size. Accordingly, the stability of CeO_2 powder dispersion was studied as a function of glycerol (dispersant) and water (dilutant) content (Table 1).

As already reported, powder dimensions are fundamental to gain slurry stability; thus, a ball-milling step was performed during slurry preparation. To evaluate ball-milling effectiveness, granulometric analyses were performed on CeO_2, both as received and after 24 h of ball milling in the dispersion medium (e.g., water and glycerol); results are reported in Figure 1.

The pristine powder (continuous line) shows a bimodal distribution centered at 2 and 0.5 μm, respectively. However, this last distribution is quite complex, evidencing a multimo-dal tail due to the presence of even smaller particles (SPs). As expected, the milling action changes powder particle size. After ball milling, indeed, the peak centered at 2 μm markedly decreases in intensity, due to a manifest comminution of the largest particles. At the same time, the peak initially centered at 0.5 μm increases in intensity and its maximum shifts at about 0.3 μm. Moreover, a decrease in distribution complexity can be detected in particular in the lower particle size region, suggesting that also smallest particles have been comminuted. A semiquantitative evaluation of particle size reduction can be assessed by calculating maxima relative ratio ($R_{LP/SM} = H_{LP}/H_{SP}$) between the larger particles (LPs) and the SPs before and after the ball-milling process. A strong comminution effect has occurred, being $R_{LP/SM}$ equal to 1.3 and 0.5 for the pristine and the ball-milled powder, respectively.

Sedimentation test is a simple but useful technique that can give qualitative or semiquantitative information on dispersion stability (Montebelli et al. 2014); for this reason, sedimentation test was applied to CeO_2 slurries prepared using different compositions.

Hence, after ball-milling step, dispersions were poured in a test tube and stability was evaluated in terms of H/H_0 ratio, as reported in the experimental part. H/H_0 values obtained as function of the settling time are plotted in Figure 2a (short term) and Figure 2b (long term).

All samples demonstrate a very good stability on both short- and long-term experiments: in the first 5 h, no apparent difference can be detected among all compositions (Figure 2a), and only slight differences arise for longer settling time due to the low glycerol/water ratio. However, this effect is less relevant considering that H/H_0 variation is in the 0.95–0.99 range, even though the glycerol/water ratio is increased to about seven times. For the experienced glycerol content, stability does not seem affected by the powder/liquid ratio, considering that this ratio was varied from 0.27 to 0.37.

Table 1. Slurry comp ositions (all values refer to 1g of cerium oxide powder; H = water, G = glycerol; samp le names refer to composition).

Sample name	Glycerol/CeO_2 (g/g)	Water/CeO_2 (g/g)	Glycerol/water
Ce_HG_1.9	1.91	1.78	1
Ce_HG_2.0	2.00	0.30	6.7
Ce_HG_2.5	2.50	0.37	6.7

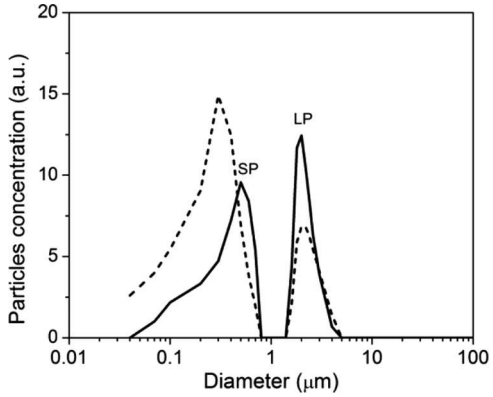

Figure 1. Particle dimension of the pristine powder (continuous) and upon 24 h of ball milling (dashed). LP: larger particles, SP: smaller particles.

The good dispersion stability also has a positive effect on slurry rheological behavior. Ce_HG_1 flow curves were selected as representative of all the samples and recorded immediately after preparation (0 h) and after 24, 48, and 72 h of in-pot ageing. Results are reported in Figure 3.

Sample immediately after the ball-milling process (Ce_HG_1-0 h) displays a typical shear-thinning behavior up to 10 s^{-1} region, while, at higher shear rates, rheology moves toward a typical Newtonian flow curve. In the Newtonian region, where a viscosity of about 0.015 Pa s is measured, both rheological behavior and viscosity are proper to be used in dip-coating technique (Cristiani et al. 2005). According to sedimentation analysis, no effect of ageing time is detected, even in the case of prolonged in-pot ageing (72 h). A nice curve overlapping is always manifest, in particular in the shear range of application (>10 s^{-1}).

A similar rheological behavior was observed by increasing the glycerol content (Table 2), as all samples preserve a Newtonian behavior at shear rates higher than 10 s^{-1}. The effect of composition is evident when considering the absolute viscosity. Indeed, increasing the glycerol/water ratio from 1 to 6.7increases the viscosity by one order of magnitude (from 0.012 to 0.13 Pa s). This effect, however, seems to reach a threshold value, considering that a further addition of glycerol with respect to powder does not affect viscosity.

On the basis of the results obtained, it can be concluded that both composition and ball-milling process are effective to obtain reasonably stable slurries with Newtonian behavior and absolute viscosities of 0.01–0.12 Pa s, in the range of shear rates of interest for the considered application. Vis-cosity can be partially modulated using the glycerol content, but in a narrow range of composition. On the contrary, an effective variation in composition in order to control vis-cosity would be useful since this parameter is of paramount importance in any coating deposition process. Indeed, it is the viscosity that determines, for instance, the final coating load, thus the layer thickness. Accordingly, other additives were experienced to properly handle slurry rheology together with glycerol.

Among other, PVA is reported to be useful for this purpose. PVA, indeed, has been widely used as a binding agent for coating production and optimization. In the literature, various examples are reported for many applications, such as low SA alumina (Khan et al. 2012), $Ce_{0.8}Sm_{0.2}O_{1.9}$ (Li 2012), $GdCeO_2$ (Akbari-Fakhrabadi et al. 2012), or other ceramic materials (Gu et al. 2012), dispersed in water liquid media.

Rheology modulation

To evaluate the possibility to control rheology via PVA addition, different dispersions were prepared (Table 3), starting from water–glycerol ratios previously discussed. In particular,

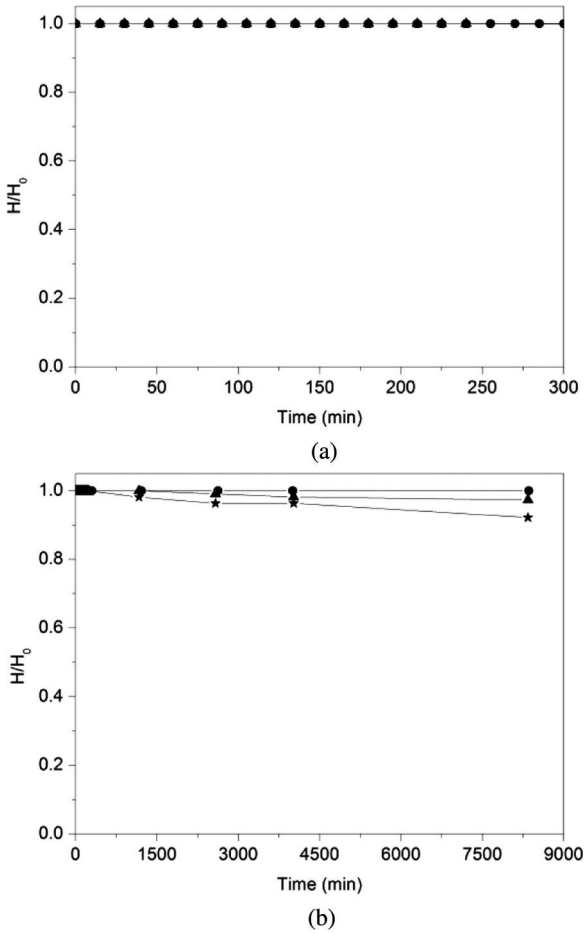

Figure 2. Sedimentation degree (H/H_0) as function of settling time: (a) short and (b) long term (star Ce_HG_1.9, triangle Ce_HG_2.0 and circle Ce_HG_2.9).

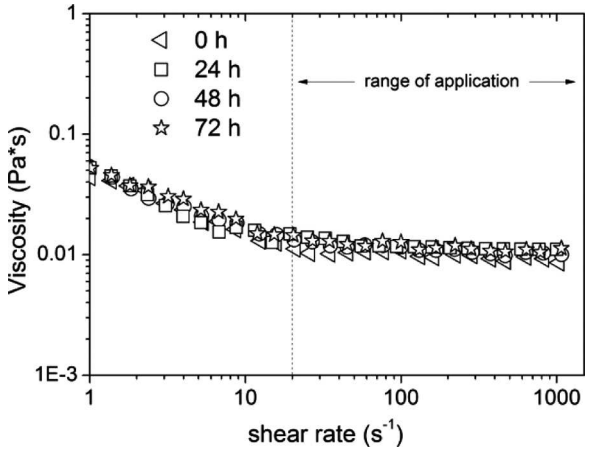

Figure 3. Flow curves of sample Ce_HG_1 as a function of ageing time.

Table 2. Slurry viscosity measured for different dispersions.

Sample name	Glycerol/CeO_2 (g/g)	η @ 20 s^{-1} (0 h) (Pa s)	η @ 100 s^{-1} (0 h) (Pa s)
Ce_HG_1.9	1.9	0.011	0.012
Ce_HG_2.0	2.0	0.13	0.12
Ce_HG_2.5	2.5	0.13	0.13

once glycerol/CeO_2 and water/CeO_2 ratios were fixed at 1.9 (g/g) and 1.8 (g/g), respectively, PVA amount was varied from 1 to 4% w/w with respect to the total liquid content (i.e., water and glycerol).

In the following, dispersions will be named composition-wise: labels contain the main components, water (H), glycerol (G), and PVA, and number related to the polymer percentage, e.g., the sample Ce_HG_PVA_1 identifies the sample containing an amount of PVA equal to 1%with respect to water and glycerol.

The effect of PVA addition on viscosity was evaluated by means of rheological measurements.

PVA content does not affect samples rheological behavior, as all of them are almost Newtonian in the considered shear-rate range. On the contrary, slurry viscosity increases by an order of magnitude with a linear dependence on increasing PVA concentration from 0.1 to 4%w/w. Results are reported in Figure 4 where viscosity at shear rate 10 s^{-1} is plotted as function of the PVA content. In this case, in the considered compositional range, no threshold effect was observed, despite the broad range of experienced composition.

Hence, rheology modulation can be quite easily achieved by properly tuning the PVA content. In addition to that, the polymer addition does not worsen slurry stability: as a matter of fact, H/H_0 values in the range 0.95–0.99 were found (Table 3).

Washcoating process

Thermal treatment: flash drying and firing

Even if rheology is the main parameter that controls the washcoating process and the final coated layers properties, thermal treatments are fundamental as well to consolidate the wet coating layer and to stick it to the support. Generally speaking, two thermal treatment steps are reported in the literature: flash drying and calcination (Valentini et al. 2001). Flash drying process is usually performed at low temperature for shorter dwelling time, with the final purpose to eliminate the dilutant and partially or totally decompose additives. In this respect, it is the key step to define the final coating adhesion and homogeneity. On the other hand, the further thermal treatment step, commonly at higher temperature, is a sort of finishing process to obtain the required structure and morphology of the coated phase

Table 3. Composition, viscosity, and stability of the dispersions as function of PVA content (*liquid = water + glycerol)

Sample name	Glycerol/CeO_2 (g/g)	Water/CeO_2 (g/g)	% PVA/liquid* (w/w)	Viscosity @ 10 s^{-1} (Pa s)	H/H0 @5000 min.
Ce_HG_PVA_0	1.9	1.8	0	0.015	0.95
Ce_HG_PVA_0.1			0.1	0.018	0.95
Ce_HG_PVA_1			1	0.029	0.96
Ce_HG_PVA_2			2	0.049	0.98
Ce_HG_PVA_4			4	0.152	0.99

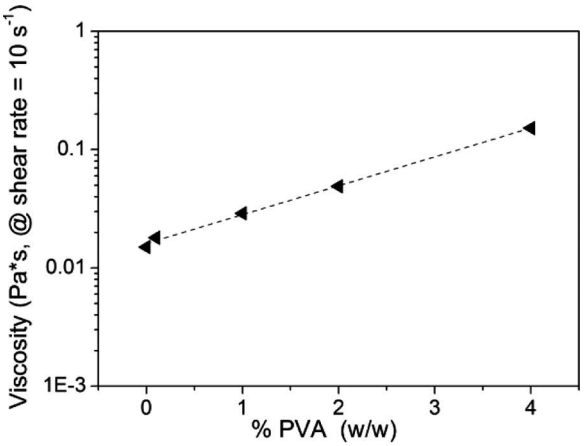

Figure 4. Viscosity (at shear rate 10 s^{-1}) as a function of the PVA content.

(Germani et al. 2007; Perego and Villa 1997). Thus, it primarily depends on the nature of the suspended powder. Even if both treatment processes have to be studied, flash drying conditions have to be carefully selected in order to achieve the targeted adhesion and homogeneity (Valentini et al. 2001).

In order to assess the optimal flash drying condition, DTA-TG analyses were performed in air on a selected slurry composition, namely Ce_HG_PVA_0.1. Results are plotted in Figure 5.

A total weight loss of about 90% is observed already at 250°C, which is attributed to water removal and to organic phase decomposition. The weight loss occurs via two main steps that can be better analyzed considering the Differential thermogravimetric (DTG) curve, where three main temperature ranges can be evidenced. In detail, the first range, from r.t. to 150°C, is characterized by a broad and complex peak centered at 70°C, due to water removal; the second one is located in the range 150–250°C where two well-defined, partially overlapped, peaks appear at 197 and 224°C; this can be attributed to glycerol decomposition in the presence of water and interacting with solid particles (Korobeinyk et al. 2013). The third one is placed above 250°C, where no decomposition phenomena occur. This last finding is quite surprising, as no evidence of PVA decomposition, which is

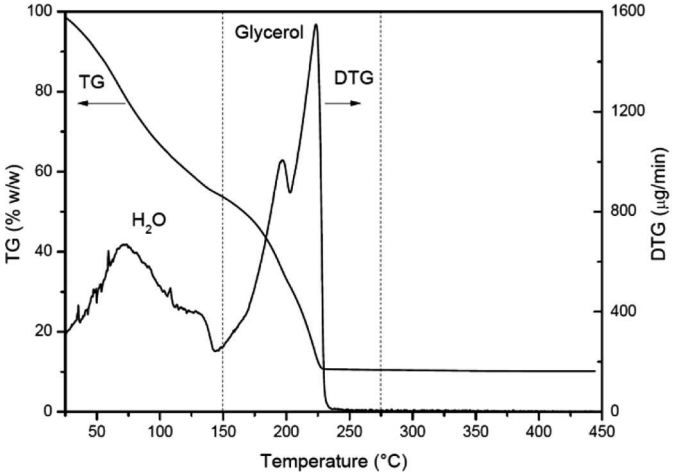

Figure 5. DTA-TG analysis in air of Ce_HG_PVA_0.1 sample.

expected to occur in the range 350–650°C, is present (Peng et al. 2005). A possible explanation for this phenomenon could be ascribed to the low PVA content of this sample (0.1%): polymer decomposition cannot be appreciated either because it is below the detection limit of the equipment or because it is anticipated due to interaction with the complex matrix. Anyway, the same behavior, here not reported, was obtained by the other formulations containing higher PVA quantities (Table 3).

On the basis of TG investigations on the slurry, 250°C was selected as flash drying step temperature. In order to verify the effectiveness of this choice in real conditions, 20 PPI foams were dip-coated using the Ce_HG_PVA_0.1 slurry, and then flash-dried at 250°C for 6 min. However, to be sure that the decomposition processes were completely finished at that temperature, also treatments at higher temperatures were experienced. In particular, the 250–500°C range (50°C steps, 6 min) was explored and effects on coated layers were evalu-ated in terms of load and adhesion. Flash drying time was set at 6 min as, for longer times, no appreciable changes on the washcoat were evidenced. Results are reported in Figure 6.

Despite DTA-TG results, a linear decrease in coating load (closed circles) was observed up to 350°C; then a constant load of about 3–3.5%is measured at higher temperatures. A similar trend was found for weight losses even if, in this case, a larger data dispersion is present, manly related to the experimental procedure for the adhesion evaluation (i.e., sonication). In any case, higher coating loads, possibly resulting in thicker layers, are less adherent to the foam surface, in line with previous results (Valentini et al. 2001; Montebelli et al. 2014). Moreover, both load and adhesion behavior suggest that DTA-TG data cannot be considered conclusive in selecting the flash drying temperature, as they suffer for the problems previously discussed. It can be concluded that flash drying temperatures lower than 350°C are not high enough to reach the total organic phase decomposition. Partial decomposition of organic additives will result in a further evolution during the following firing step at higher temperature; this could result in a worsening of the coating, determining surface cracking and coating detachment. On this basis, all samples were flash dried at 350°C.

Moreover, it has to be noted that, after the flash drying process, no pore clogging is detected, to confirm the effectiveness of the selected operating conditions.

The operating parameters of the firing step, 900°C and dwelling time of 10 h, were selected to be representative not only of mild but also of strong operation processes.

Effect of slurry viscosity

As previously discussed, slurry viscosity can be tuned by controlling PVA concentration. Accordingly, the effect of slurry rheological properties on final coating quality was investigated using the slurry composition at increasing PVA content of Table 2 and 20 PPI foams. Results are reported in Figure 7, where load dependence on viscosity (at shear rate $10\,s^{-1}$) is displayed.

As expected, coating load clearly depends on viscosity: the higher the viscosity, the higher the average loading on foams. However, such a dependence is more marked in the first part of the curve: indeed, a sharp increase is observed at lower viscosities, while the trend becomes smoother, apparently approaching a threshold value. The increase in viscosity is directly related to the PVA content, as already pointed out. However by increasing the PVA content forty times (from 0.1 to 4%), the viscosity is increased only by one order of magnitude (from 0.018 to 0.16 Pa s) and the final coating load is not even doubled (from 3.5 to 4.5). This suggests that high coating load cannot be obtained via viscosity management.

Regarding coating adhesion, the expected correlation load and adhesion was not found (Figure 8) for these samples. It is well known that lower adhesion is related to thicker layers (Valentini et al. 2001; Montebelli et al. 2014). Very scattered values are measured, also characterized by large error ranges, which cannot allow any speculation on them. The behavior is hard to be understood, as there is no chemical reason for that. A possible explanation can be found considering foam nature: indeed, ceramic foams are very brittle and, in some cases, they were damaged during adhesion tests. Accordingly, the observed irreproducibility or scattering of weight loss results are possibly due to foam scraps formed randomly. In addition to that, the volcano shape curve may be ascribed to

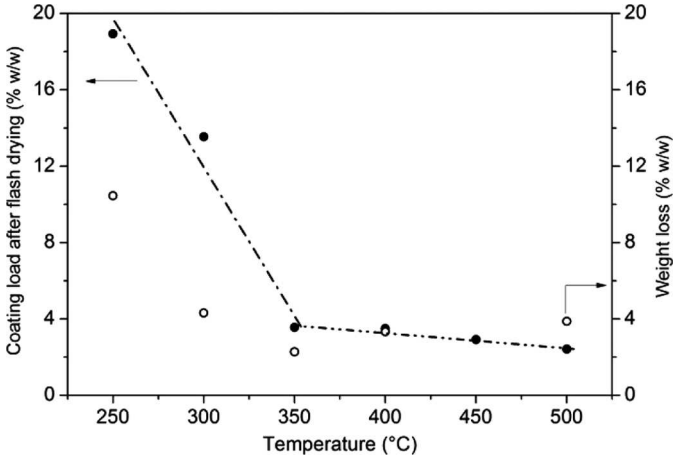

Figure 6. Coating load (closed circles) and weight loss (op en circles) of 20 PPI foams coated with Ce_HG_PVA_0.1 as a function of the flash drying temperature.

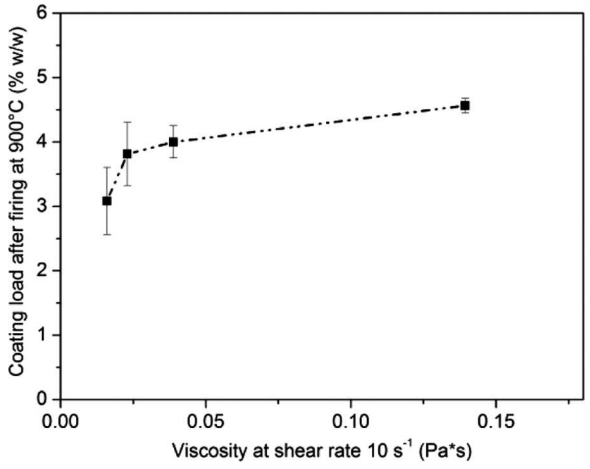

Figure 7. Coating load after firing as a function of viscosity at shear rate $10\,s^{-1}$.

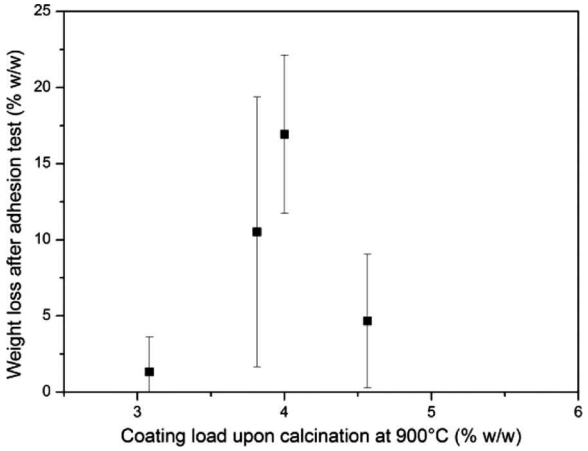

Figure 8. Weight loss after adhesion test as a function of the coating load for Ce_HG_PVA_0.1 fired at 900°C.

the superposition of two different phenomena: an increase in PVA content leads to higher load and thus to higher losses; at the same time, an increase in binder content decreases the capillary forces during drying, leading to more homogeneous and adherent crack-free layers. For these reasons, it is not possible to identify a clear relation between losses and viscosity, and thus between loading and PVA content. Alternative experiments should be carried out in order to measure real coating adhesion.

The effect of viscosity was also evaluated with respect to surface morphology and homogeneity. Coated samples were characterized by means of optical microscopy. Pictures of foams coated with formulations of different PVA content, namely 2 (η @10 $s^{-1} \approx 0.05$ Pa s) and 4% w/w (η @10 $s^{-1} \approx 0.15$ Pa s), respectively, are compared in Figure 9.

Despite a poor coverage of the support, both samples display the presence of the oxide layer spread on the foam surface. Furthermore, no pore clogging occurred using both dispersions (Figure 9). For samples prepared with the higher organic amount, an extended surface darkening was present upon flash drying at 350°C, which could probably be inquired to PVA partial decomposition to give carbon residuals. After heat treatment at 900°C for 10 h, surface darkening is removed, pointing out how the total organic residue decompo-sition is reached at that temperature. Furthermore, these optical microscope images confirm the scarse effect of vis-cosity on load. Indeed, comparable foams coverages were found for samples coated with slurries of different viscosity.

On this basis, alternative parameters were studied in order to obtain a homogeneous and complete surface coverage.

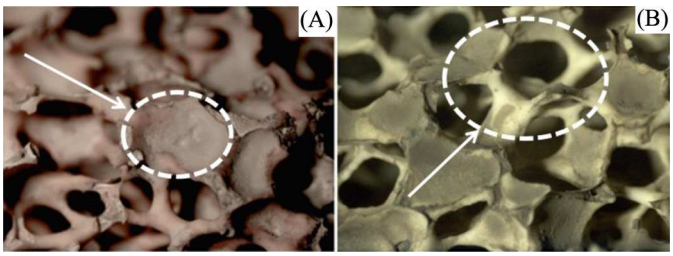

Figure 9. Optical microscope images of S20_HG_PVA_2 (A) and S20_HG_PVA_4 (B), upon firing at 900°C (15 × magnification).

Withdrawal velocity

In literature, coating load and wet-layer thickness dependence on withdrawal velocity has been widely investigated (Middleman 1977; Zhang et al. 2012). In order to verify this effect using the previously introduced formulations, some 20 PPI open-cell foams were coated with the Ce_HG_PVA_0.1 slurry, which showed a Newtonian behavior at shear rate higher than 10 s^{-1} and a viscosity of 0.018 Pa s (Table 3). During deposition, five different withdrawal velocities were tested, i.e., 34, 31, 25, 13, and 6 cm min^{-1}. Results evaluated in terms of coating load after the firing process at 900°C pointed out that there is no effect of withdrawal velocity on coating load, despite the broad speed range explored. Load was found to be 3.1 wt.% "plus or minus" 0.4 wt.%. This result is in accordance with the observed Newtonian behavior of the slurry in the typical shear rate here applied. On the basis of these results, withdrawal velocity was set constant at 13 cm min^{-1}.

Effect of the dipping number

To evaluate the possibility to manage coating load by means of multiple depositions, all the different slurries (that are Ce_HG_PVA_0.1-4) were used to dip-coat one (one deposition, 1D), two (2D), and three (3D) times the 20 PPI foams. After each deposition, a flash drying step was carried out at 350°C and the final thermal treatment was performed at 900°C. Despite some misleading points, a trend in loading can be evidenced as a function of dipping numbers (Figure 10). Almost similar amounts of coating are deposited at any step, corresponding to approximately 2.5%(w/w) and 3–4% (w/w) per step, respectively, when lower and higher viscosities were used. The differences observed from 1D, 2D, and 3D loads can be ascribed to different starting surfaces. In the first deposition, substrate is the bare foam surface, while in the second and third ones it is the already coated layer, with different nature and pore dimensions.

Anyway, the possibility to operate via multiple dipping allows the achievement of quite high coating loads, from 2 to 12% w/w, which should guarantee a better coverage of the foam surface.

This result points out how, via multiple dipping, a good coverage can be obtained even in the case of low viscosity

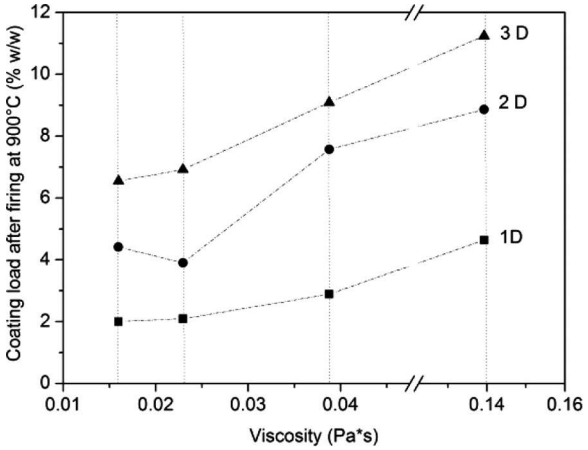

Figure 10. Coating load after calcination as a function of viscosity and dipping numbers (lines are drawn as guide for the eyes).

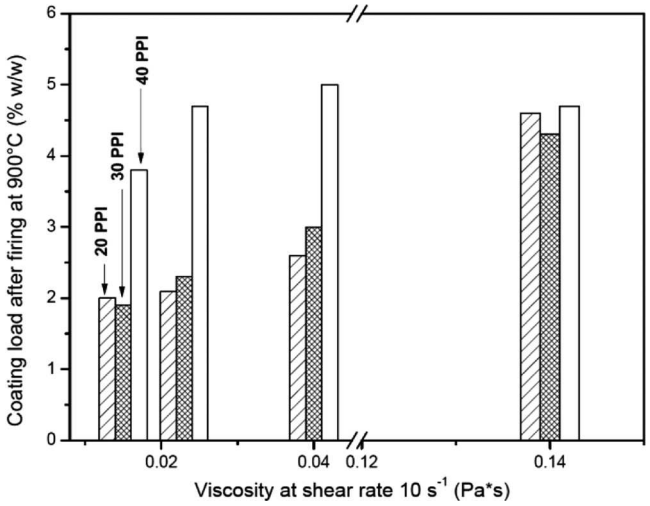

Figure 11. Coating load after firing at 900°C of foams with different PPI as function of viscosity.

slurries, thus avoiding instability or rheological problems arising from highly viscous systems and/or high powder concentrations. However, also in this case, scatter data on adhesion were found with losses in the 3–10% w/w range. Anyway, as already observed, the contribution of some foam scraps to the total weight losses cannot be excluded.

Effect of the pore density

Pore density effect was evaluated comparing 20, 30, and 40 PPI foams. For each porosity, the four different PVA-based slurries were used (refer to Table 3 for composition details). Five sam-ples were prepared for each pore density/ composition combi-nation, in order to evaluate results and their reproducibility. In Figure 11, average coating deposition amounts are reported as a function of the slurry viscosity. 20 PPI samples, already discussed, are reported for comparison.

Once the viscosity value was fixed, a market effect of foam PPI was evident, particularly at lower viscosities: the coating load of 40 PPI foam is at least the double that of 20 and 30 PPI samples, possibly due to a different path of the slurry in smaller struts. However, once viscosity is increased at 0.14 Pa s, all samples behaved in the same manner and the effect of slurry rheology prevails on pore density. Standard deviations in the order of 0.2–0.6%were found; accordingly data fluctuation on loads could be ascribed to experimental errors. However, for all the samples, a quite homogeneous coverage was observed when coated with the 0.14 Pa s slurry, and, more important, very little or at least no pore clogging was observed, even for the 40 PPI foam.

Also in this case, a scarce meaning was found in the adhesion test results, as highly scattered weight losses in the 2–10% (w/w) range were detected. Moreover, weight losses are totally independent on coating load or on strut dimensions; further investigations need to be accomplished.

30 PPI foam washcoated by using Ce_HG_PVA_0.1 slurry was characterized by Scanning Electron Microscopy (SEM) analysis. Results are reported in Figure 12. In the first row (a and c), flash dried surface after one dipping is reported at different magnifications while pictures reported in Figure 12b and d represent the bare ceramic foam surface. By comparing coated and uncoated samples, the finely textured cerium oxide layer appears to be homogeneous and only few areas are not completely covered. The local lack of homogeneity can be easily fixed by performing multiple depositions or by using a formulation based on higher PVA concentration.

Conclusions

1. *Slurry stability and rheology*—The acid-free formulation based on water, glycerol, and PVA is effective to disperse and to stabilize, via steric-like interaction, low SA powders, such as cerium oxide. In addition to that, milling process has been confirmed to be helpful to improve dispersion stability.

From a rheological point of view, proper ratios among components allow slurry rheology tuning. Newtonian fluids,

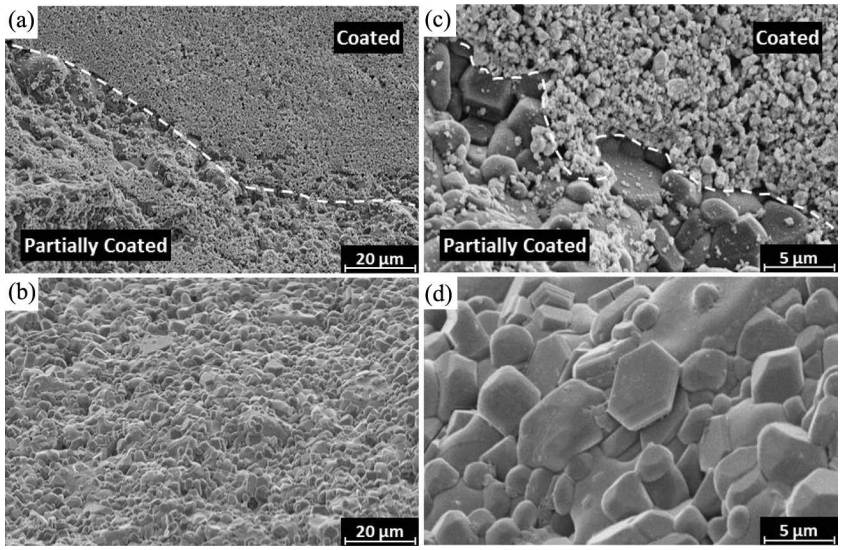

Figure 12. SEM analysis for coated (a and c) and bare (b and d) 30 PPI foams at different magnifications.

in the range of shear of application, are obtained, suitable for the dip-coating process of the foams. PVA can be used as viscosity modulator: the higher the PVA content, the higher the viscosity of the system.

2. *Washcoating operating parameters*—Withdrawal velocity does not affect deposition: a constancy of coating load is obtained, once rheological properties were fixed. On the other hand, multiple dipping is an effective way to enhance coating load. Also in multiple dipping process, rheology is the key parameter: at fixed viscosity almost the same amount of coating is loaded at each dipping step.

Foams of different porosity (20, 30, and 40 PPI) can be coated without changes on slurry formulation. Good coverage with no pore clogging has been obtained for all samples, using all the slurry formulation here adopted.

3. *Thermal treatments* – 350°C was identified as the optimal flash drying temperature to consolidate the coated layer and to decompose the organic additives at the same time. Good results have been obtained in terms of coating load after calcinations at 900°C, while, even though acceptable weight loss at least of 10% was obtained, further investigations need to be accomplished to understand scattering of adhesion test data.

Funding

The authors acknowledge the "Intensification of Catalytic Processes for Clean Energy, Low-Emission Transport and Sustainable Chemistry using Open-Cell Foams as Novel Advanced Structured Materials" project (MIUR, PRIN, Italy) for financial support.

References

Aegerter, M. A., and M. Mennig. 2004. *Sol–gel technologies for glass producers and users*. Boston, MA, USA: Kluwer Academic Publishers.

Agrafiotis, C., A. Tsetsekou, and A. Ekonomakou. 1999. The effect of particle size on the adhesion properties of oxide washcoats on cordierite honeycombs. *Journal of Materials Science Letters* 18 (17):1421–24.

Akbari-Fakhrabadi, A., R. V. Mangalaraja, F. A. Sanhueza, R. E. Avila, S. Ananthakumar, and S. H. Chan. 2012. Nanostructured Gd-CeO2 electrolyte for solid oxide fuel cell by aqueous tape casting. *Journal of Power Sources* 218:307–12. doi:10.1016/j.jpowsour.2012.07.005.

Bravo, J., A. Karim, T. Conant, G. P. Lopez, and A. Datye. 2004. Wall coating of a CuO/ZnO/Al2O3 methanol steam reforming catalyst for microchannel reformers. *Chemical Engineering Journal* 101 (1–3):113–21. doi:10.1016/j.cej.2004.01.011.

Brinker, C. J., and G. W. Scherer. 1990. *Sol–gel science: The physics and chemistry of sol–gel processes*. New York, NY: Academic Press.

Cristiani, C., E. Finocchio, S. Latorrata, C. G. Visconti, E. Bianchi, E. Tronconi, G. Groppi, and P. Pollesel. 2012. Activation of metallic open-cell foams via washcoat deposition of Ni/MgAl2O4 catalysts for steam reforming reaction. *Catalysis Today* 197 (1):256–64. doi:10.1016/j.cattod.2012.09.003.

Cristiani, C., M. Valentini, M. Merazzi, S. Neglia, and P. Forzatti. 2005. Effect of ageing time on chemical and rheological evolution in gamma-Al2O3 slurries for dip-coating. *Catalysis Today* 105 (3–4):492–98. doi:10.1016/j.cattod.2005.06.020.

Cristiani, C., C. G. Visconti, E. Finocchio, P. G. Stampino, and P. Forzatti. 2009. Towards the rationalization of the washcoating process conditions. *Catalysis Today* 147:S24–9. doi:10.1016/j.cattod.2009.07.031.

Germani, G., A. Stefanescu, Y. Schuurman, and A. C. van Veen. 2007. Preparation and characterization of porous alumina-based catalyst coatings in microchannels. *Chemical Engineering Science* 62 (18–20): 5084–91. doi:10.1016/j.ces.2007.02.034.

Gu, S. I., H. S. Shin, D. H. Yeo, and S. Nahm. 2012. The effects of the particle size and organic content of YSZ on sheet properties. *Journal of Ceramic Processing Research* 13 (5):556–60.

Gu, Y., C. Q. Xia, F. H. Zeng, and C. B. Liu. 2003. Stabilized dispersion of nano-ceramic coating. *Transactions of Nonferrous Metals Society of China* 13 (4):890–92.

Hosokawa, S., M. Taniguchi, K. Utani, H. Kanai, and S. Imamura. 2005. Affinity order among noble metals and CeO2. *Applied Catalysis A: General* 289 (2):115–20. doi:10.1016/j.apcata.2005.04.048.

Khan, A. U., N. Mahmood, and P. F. Luckham. 2012. Rheological characterization of alumina ceramic suspensions in presence of a dispersant and a binder. *Journal of Dispersion Science and Technology* 33 (8):1210–17. doi:10.1080/01932691.2011.605646.

Korobeinyk, A. V., R. B. Kozakevych, Yu. M. Bolbukh, and V. A. Tertykh. 2013. Microwave assisted carbonization of glycerol on silica surface. *Chemistry, Physics and Technology of Surface* 4 (1):55–61.

Li, X. 2012. Aqueous tape casting of SDC with a multifunctional dispersant. *Journal of Ceramic Processing Research* 13 (3):324–29.

Maupin, I., J. Mijoin, J. Barbier, N. Bion, T. Belin, and P. Magnoux. 2011. Improved oxygen storage capacity on CeO2/zeolite hybrid catalysts. Application to VOCs catalytic combustion. *Catalysis Today* 176 (1):103s–09. doi:10.1016/j.cattod.2011.02.003.

Meille, V. 2006. Review on methods to deposit catalysts on structured surfaces. *Applied Catalysis A: General* 315:1–17. doi:10.1016/j.apcata.2006.08.031.

Meille, V., S. Pallier, G. V. Santa Cruz Bustamante, N. Roumanie, and J. P. Reymond. 2005. Deposition of gamma-Al2O3 layers on structured supports for the design of new catalytic reactors. *Applied Catalysis A – General* 286 (2):232–38. doi:10.1016/j.apcata.2005.03.028.

Middleman. 1977. *Fundamentals of polymers processing*. New York, NY, USA: McGraw-Hill.

Montebelli, A., C. G. Visconti, G. Groppi, E. Tronconi, C. Cristiani, C. Ferreira, and S. Kohler. 2014. Methods for the catalytic activation of metallic structured substrates. *Catalysis Science & Technology* 4:2846–70. doi:10.1039/C4CY00179F.

Peng, Z., L. X. Kong, and S. D. Li. 2005. Study on thermooxidative degradation of poly(vinyl alcohol)/silica nanocomposite prepared with SAM technique. *Journal of Metastable and Nanocrystalline Materials Series* 23:375–78 [edited by Gupta, M. and Lim, C.Y.H.]. doi:10.4028/www.scientific.net/jmnm.23.375

Perego, C., and P. Villa. 19 9 7.Catalyst preparation methods. *Catalysis Today* 34 (3–4):281–305. doi:10.1016/s0920-5861(96)00055-7.

Phan, X. K., H. Bakhtiary-Davijany, R. Myrstad, P. Pfeifer, H. J. Venvik, and A. Holmen. 2011. Preparation and performance of Cu-based monoliths for methanol synthesis. *Applied Catalysis A: General* 405 (1–2):1–7. doi:10.1016/j.apcata.2011.07.005.

Rodriguez, P., V. Meille, S. Pallier, and M. A. Al Sawah. 2009. Deposition and characterisation of TiO2 coatings on various supports for structured (photo)catalytic reactors. *Applied Catalysis A: General* 360 (2): 154–62. doi:10.1016/j.apcata.2009.03.013.

Shan, W., M. Luo, P. Ying, W. Shen, and C. Li. 2003. Reduction property and catalytic activity of Ce1 − XNiXO2 mixed oxide catalysts for CH4 oxidation. *Applied Catalysis A: General* 246 (1):1–9. doi:10.1016/s0926-860x(02)00659-2.

Tronconi, E., and G. Groppi. 2009. 3rd international conference on structured catalysts and reactors. *Catalysis Today* 147:S1.

Valentini, M., G. Groppi, C. Cristiani, M. Levi, E. Tronconi, and P. Forzatti. 2001. The deposition of gamma-Al2O3 layers on ceramic and metallic supports for the preparation of structured catalysts. *Catalysis Today* 69 (1–4):307–14. doi:10.1016/s0920-5861(01)00383-2.

Visconti, C. G., E. Tronconi, L. Lietti, G. Groppi, P. Forzatti, C. Cristiani, R. Zennaro, and S. Rossini. 2009. An experimental investigation of Fischer-Tropsch synthesis over washcoated metallic structured supports. *Applied Catalysis A: General* 370 (1–2):93–101. doi:10.1016/j.apcata.2009.09.023.

Vita, A., G. Cristiano, C. Italiano, L. Pino, and S. Specchia. 2015. Syngas production by methane oxy-steam reforming on Me/CeO2 (Me = Rh, Pt, Ni) catalyst lined on cordierite monoliths. *Applied Catalysis B: Environmental* 162:551–63. doi:10.1016/j.apcatb.2014.07.028.

Won, J. Y., H. K. Jun, M. K. Jeon, and S. I. Woo. 2006. Performance of microchannel reactor combined with combustor for methanol steam reforming. *Catalysis Today* 111 (3–4):158–63. doi:10.1016/j.cattod.2005.11.004.

Zhang, H., W. J. Suszynski, K. V. Agrawal, M. Tsapatsis, S. Al Hashimi, and L. F. Francis. 2012. Coating of open cell foams. *Industrial & Engineering Chemistry Research* 51 (27):9250–59. doi:10.1021/ie300266p.